S1P in HDL promotes interaction between SR-BI and S1PR1 and activates S1PR1-mediated biological functions: calcium flux and S1PR1 internalization[s]

Mi-Hye Lee,* Kathryn M. Appleton,[†] Hesham M. El-Shewy,* Mary G. Sorci-Thomas,[§] Michael J. Thomas,[§§] Maria F. Lopes-Virella,*[,**] Louis M. Luttrell,*[,†,**] Samar M. Hammad,[††,1] and Richard L. Klein*[,**,1,2]

Division of Endocrinology, Metabolism, and Medical Genetics, Department of Medicine,* Department of Pharmaceutical & Biomedical Sciences,[†] College of Pharmacy, and Department of Regenerative Medicine and Cell Biology,[††] Medical University of South Carolina, Charleston, SC; Division of Endocrinology, Metabolism, and Clinical Nutrition, Department of Medicine,[§] and Department of Pharmacology and Toxicology,[§§] Medical College of Wisconsin, Milwaukee, WI; and Research Service,** Ralph H. Johnson Department of Veterans Affairs Medical Center, Charleston, SC

Abstract HDL normally transports about 50–70% of plasma sphingosine 1-phosphate (S1P), and the S1P in HDL reportedly mediates several HDL-associated biological effects and signaling pathways. The HDL receptor, SR-BI, as well as the cell surface receptors for S1P (S1PRs) may be involved partially and/or completely in these HDL-induced processes. Here we investigate the nature of the HDL-stimulated interaction between the HDL receptor, SR-BI, and S1PR1 using a protein-fragment complementation assay and confocal microscopy. In both primary rat aortic vascular smooth muscle cells and HEK293 cells, the S1P content in HDL particles increased intracellular calcium concentration, which was mediated by S1PR1. Mechanistic studies performed in HEK293 cells showed that incubation of cells with HDL led to an increase in the physical interaction between the SR-BI and S1PR1 receptors that mainly occurred on the plasma membrane. Model recombinant HDL (rHDL) particles formed in vitro with S1P incorporated into the particle initiated the internalization of S1PR1, whereas rHDL without supplemented S1P did not, suggesting that S1P transported in HDL can selectively activate S1PR1. JLR In conclusion, these data suggest that S1P in HDL stimulates the transient interaction between SR-BI and S1PRs that can activate S1PRs and induce an elevation in intracellular calcium concentration.—Lee, M.-H. K.M. Appleton, H.M. El-Shewy, M.G. Sorci-Thomas, M.J. Thomas, M.F. Lopes-Virella, L.M. Luttrell, S.M. Hammad, and R.L. Klein. **S1P in HDL promotes**

The reverse transport of cholesterol from the periphery to the liver is often considered as the hallmark antiatherogenic function of HDL. SR-BI, the first molecularly characterized HDL receptor that plays a critical role in this metabolism, is abundantly expressed in several types of cells and tissue types, including the liver parenchyma, adrenal cortical cells, platelets, endothelial cells, smooth muscle cells, and macrophages. SR-BI facilitates the selective uptake of HDL cholesterol by cells, primarily in the form of cholesteryl esters. SR-BI also mediates the bidirectional flux of unesterified cholesterol and phospholipids between HDL and cells, which leads to an increase in cellular cholesterol mass and alters cholesterol distribution in plasma membrane domains (1–4).

Numerous studies have detailed the various signaling pathways generated by the interaction of HDL with cell surface receptors that have been shown to induce myriad

biological responses, including inhibition of lipid oxidation, impairment of leukocyte adhesion and monocyte activation, increased nitric oxide production, prostacyclin synthesis and flow-induced vasodilation, and the prevention of endothelial cell damage and death (5–8). Studies have also shown that HDL can inhibit synthesis of matrix metalloproteinases, promote smooth muscle cell proliferation, and inhibit activation of platelets and the coagulation cascade (9). Recent studies using a variety of experimental approaches have concluded that the SR-BI receptor and the sphingosine 1-phosphate receptors (S1PRs) may interact to mediate these HDL-induced process (10–12).

HDL is the most prominent plasma carrier of sphingosine 1-phosphate (S1P) (more than 50% of lipoprotein-associated S1P found in HDL). The small, dense HDL particles, HDL3, carry 2- to 3-fold higher S1P levels compared with HDL2 on a molar basis (13–16). It has been shown previously that several biological effects that are ascribed to HDL may be mediated by the S1P content of HDL through activation of S1PRs. S1P in HDL has been shown to mediate several antiatherogenic functions by activating numerous signaling pathways through stimulation of multiple signaling pathways, including PKC, PI3-K/Akt, p38 MAPK, p42/44ERK1/2, and the Rho/Rho kinase pathways (17–19).

Previous studies have focused on the individual involvement of either the SR-BI or S1PR receptor proteins in HDL-mediated biological effects or signaling pathways, but studies investigating the potential for both receptors to jointly mediate HDL-induced biological functions are limited (20, 21). We have previously shown that HDL mediates plasminogen activator inhibitor-1 secretion in 3T3L1 adipocytes through activation of S1PR2 (16) and determined that SR-BI is also required to affect this metabolism (unpublished observation). It has been hypothesized that the binding of HDL to the SR-B1 receptor may provide the necessary spatial geometry to bring HDL-bound S1P sufficiently close to its cognate receptors to initiate the various S1PR-mediated signaling cascades on the cell surface (20, 22). However, there are no experimental data to support this hypothesis. Here we report the nature of the physical interactions between the HDL receptor, SR-BI, and the S1P-binding receptor, S1PR1, using a protein-fragment complementation assay (PCA) and confocal microscopy. The efflux of intracellular calcium and the internalization of S1PR1 receptors were investigated as representative biological functions that are modified by HDL-bound S1P, which is delivered to the cell as a result of the cooperative interaction of these cell receptors.

MATERIALS AND METHODS

Materials

Pertussis toxin (PTX) was obtained from Calbiochem-EMD Biosciences Inc. (San Diego, CA). The S1PR2 antagonist JTE-013 and the S1PR1/S1PR3 inhibitor VPC23019 were purchased from Cayman Chemical (Ann Arbor, MI) and Avanti Polar Lipids, Inc. (Alabaster, AL). S1P was purchased from Avanti Polar Lipids. Fu-Gene HD transfection reagent was obtained from Fisher Scientific

(Pittsburgh, PA). FLIPR Calcium 5 Assay Kit was from Molecular Devices, Inc. (Downingtown, PA). Cell culture medium and cell culture additives were from Life Technologies (Grand Island, NY). Human scavenger receptor class B member 1 cDNA was obtained from ORIGENE (Rockville, MD). The pEGFP-N1-myc-S1PR1 plasmid was a generous gift from Dr. Timothy Palmer (Institute of Biomedical and Life Sciences, University of Glasgow, UK) (23). Venus yellow fluorescent protein (YFP) PCA plasmid DNAs were a generous gift from Dr. Stephen Michnick (University of Montreal, Quebec, Canada). pEGFPC3, pEYFP-N1, and pmCherry-N1 were obtained from Clontech (Mountain View, CA). SR-BI siRNA was obtained from Santa Cruz Biotechnology Inc. (Dallas, TX). Palmitoyloleoyl phosphatidylcholine (POPC), D-erythro-sphingosine-1-phosphate, D-erythro-sphingosine-1-phosphate, and D-erythro-sphingosine were purchased from Avanti Polar Lipids (Alabaster, AL).

Isolation of HDL2 and HDL3

HDL2 and HDL3 were isolated from plasma as we described previously (16). Briefly, blood (200 ml) was collected in the presence of an anticoagulant/lipoprotein preservative cocktail [EDTA (0.1% w/v), chloramphenicol (20 μg/ml), gentamycin sulfate (50 μg/ml), epsilon-α-caproic acid (0.13% w/v), and dithiobisnitrobenzoic acid (0.04% w/v) to inhibit LCAT activity (final concentrations)] after an overnight fast from each of three or four donors who were free from clinically apparent disease. Blood was then centrifuged (2800 g, 20 min, 4°C) to obtain plasma. HDL2 (1.063 < d < 1.125 g/ml) and HDL3 (1.125 < d < 1.21 g/ml) were isolated by sequential ultracentrifugation of plasma with density adjusted with solid KBr in a Ti70 rotor (Beckman-Coulter Instruments, Palo Alto, CA) spun at 70,000 rpm for 18 h at 4°C. The floating HDL subfractions were harvested after tube slicing, and each isolated HDL subfraction was washed and concentrated by ultracentrifugation at its isolation density in a in a SW41 rotor (41,000 rpm, 36 h, 4°C). HDL subfractions were dialyzed against saline/EDTA (150 mM NaCl, 300 μM EDTA; pH 7.4), sterilized by filtering through a 0.22 μm membrane, and stored at 4°C until used. Each participant provided written informed consent, and the Institutional Review Board of the Medical University of South Carolina approved the experimental protocol.

Synthesis of recombinant HDL and recombinant HDL containing S1P

Recombinant HDL (rHDL) was formulated in vitro using a molar ratio of 80:1 of POPC to apoA-I, as previously described (24). Lipid-free human apoA-I was purified from HDL isolated by sequential ultracentrifugation plasma as described (25). Final purity was assessed by mass spectrometry (26). Briefly, POPC dissolved in chloroform was dried onto the side of a glass tube and then dried overnight under vacuum. Next, a 2-fold molar excess of sodium cholate, dissolved in 10 mM Tris (pH 7.4), was added to the tube of POPC and incubated for 1 h at 37°C with shaking. Once the lipid was removed from the side of the tube, the mixture was agitated on a mechanical vortexer for 1–2 h at room temperature. An aliquot of human plasma apoA-I was added to the lipid micelle mixture to achieve a molar ratio of 80:1 POPC/apoA-I, mixed gently, and then dialyzed against 10 mM ammonium bicarbonate (pH 7.4) at room temperature. Dialysis continued until all sodium cholate was removed. rHDL particle size and homogeneity were determined by 4–30% nondenaturing gradient gel electrophoresis stained with Coomassie Blue and compared with high-molecular-weight standards of known Stokes' diameter, as previously described (27).

rHDL preparations also were formulated to contain sphingosine-1-phosphate (rHDL + S1P) at a starting molar ratio of

80:0.07:1 of POPC/S1P/apoA-I. Briefly, S1P was dissolved in a 3:3:1 (v/v) of chloroform/methanol/water and then sonicated at 50°C for 1 h in a tightly capped glass tube. An aliquot of the dissolved S1P was removed and then dried onto the side of a glass tube containing POPC, and rHDL were formulated as described above. After purification of the rHDL containing S1P, aliquots were taken for quantification of the final S1P concentration in rHDL using mass spectrometry.

Quantification of S1P in rHDL using mass spectrometry

S1P concentrations were measured essentially as described by Berdyshev et al. (28) containing 50 pmol of $C^{17}S1P$ as an internal standard. After extraction and derivatization, bisacetylated S1P was analyzed on an YMC-Pack ODS-AQ column (YMC) (100×1.0 mm inner diameter, 3-μm particle size) and detected using a TSQ Quantum Discovery Max Triple Quadrupole mass spectrometer (ThermoFinnigan, San Jose, CA) in negative ion mode. Bisacetylated sphingolipids were eluted using the following gradients: 2 min hold of solvent A/solvent B (50:50), ramp to 100% solvent B over 0.1 min, hold at 100% solvent B for 8.5 min, and then regenerate the column with solvent A/solvent B (50:50) for 30 min with the following settings: ion spray voltage -3000 V, ion transfer capillary temperature 200°C, collision gas 1 millitorr of argon with a collision energy of 11 V. Multiple reaction monitoring transitions monitored were C17S1P m/z 448/388 and S1P m/z 462/402.4 (29).

Cells

Primary rat aortic vascular smooth muscle (RVSM) cells were isolated from 75–100 g Sprague-Dawley rats (Charles River Laboratories, Wilmington, MA) as previously described (30). RVSM cells were maintained in minimum essential medium (MEM) (Invitrogen, Grand Island, NY) supplemented with 10% FBS and 1% antibiotic/antimycotic solution (Sigma Chemical Co., St. Louis, MO). Cells were fed every 2 days and subcultured upon reaching 90% confluence. Prior to each experiment, cells were seeded into black-wall, clear-bottom 96-well plates and incubated for 24 h in serum-free growth medium supplemented with 0.1% BSA and 1% antibiotic/antimycotic solution. All experiments on RVSM cells were performed between passages four and nine. HEK293 cells were maintained in MEM supplemented with 10% FBS and 1% antibiotic/antimycotic solution. Prior to experimentation, cells were serum deprived overnight or for 4–6 h in serum-free growth medium supplemented with 0.1% BSA and 1% antibiotic/antimycotic solution.

Plasmid DNA constructs

The plasmid DNAs coding for human, GFP-tagged, SR-BI were constructed using PCR with two primers (hSRBI-*Hin*dIII: ATCAAGCTTATGGGCTGCTCCGCCA and hSRBI-*Kpn*I: GCGGTACCCTACAGTTTTGCTTCCTG). PCR products containing human SR-BI were digested with *Hin*dIII and *Kpn*I and inserted into linearized pEGFPC3.

To generate the human, S1PR1-YFP, and S1PR1-Cherry plasmid cDNAs, pEGFP-N1-myc-S1PR1 was digested with *Hin*dIII and *Apa*I to form S1PR1 cDNAs. These DNA fragments were ligated with linearized pEYFP-N1 or pmCherry-N1. To construct the cDNA containing human SR-BI complexed to the Venus-1 fluorophore, the cDNA containing S1PR1 complexed with either the Venus-1 or Venus-2 fluorophore, and the cDNA containing the parathyroid hormone receptor 1 (PTH1R) complexed to the Venus 2 fluorophore, the following two sets of primers were used in the PCR reaction: hSRBI-Not: AGGCGGCCGCACCATGGGCTGCTCCGCCA, hSRBI-*Cla*I: CCATCGATCAGTTTTGCTTCCTGCAGCACAGAG, hS1PR1-Not: AGGCGGCCGCACCATGGG-

GCCCACCAGCGT, hS1PR1-ClaI: CCATCGATGGAAGAAGAGTTGACGTTTCCAGAAG, hPTH1R-NotF: AGGCGGCCGCACCATGGGGACCGCCCGGA, and hPTH1R-ClaR: CCATCGATCATGACTGTCTCCCACTCTTCCTGTAG. DNA sequencing was performed to verify the correct reading frame in each plasmid DNA construct.

Assay of calcium flux using FLIPR^{TETRA}

RVSM and HEK293 cells were seeded on clear bottomed, black-walled 96-well plates and grown until subconfluent. To investigate the influence of SR-BI expression level on HDL-mediated calcium influx, HEK293 cells were transiently transfected with either 1.5 μg of SR-BI plasmid DNAs for overexpression, or with 20 nM of siSR-BI for downregulation of SR-BI using the Fu-Gene HD and GeneSilencer transfection reagents, respectively, with minor alterations to the manufacturers' recommendations. The next day, the cells were seeded on collagen-coated, clear-bottomed, black-wall 96-well plates. At 48 h after the transient transfections, the cells were serum starved for 3–4 h in MEM supplemented with 0.1% FBS. A 100 μl aliquot of FLIPR 5 calcium-sensitive dye was added to 100 μl serum deprivation medium, and the cells were incubated for an additional 1 h at 37°C and 5% CO_2. Experiments were conducted using a FLIPR^{TETRA} instrument (Molecular Devices, Sunnyvale, CA) as previously described (31) using a 470–495 nm excitation and a 515–575 nm emission filter installed prior to initializing the FLIPR^{TETRA}. All assays were conducted at room temperature. The instrument was programmed to simultaneously dispense 50 μl of vehicle control, 5× ligand, or the calcium ionophore A23187 from the drug plate into the 200 μl of medium in the corresponding wells of the assay plate to achieve the final ligand concentration.

Analysis of the cellular distribution of the SR-BI and S1PR1 receptors using confocal microscopy

HEK293 cells were plated onto collagen-coated, 35-mm glass-bottom dishes (MatTek Corp., Ashland, MA). The cultured cells were transiently transfected with 0.7 μg of GFP-tagged SR-BI and 0.1 μg of Cherry-tagged S1PR1 DNAs using the FuGene HD reagent. Thirty-six hours after transfection, cells were deprived of serum for 4 h and then stimulated with agonists for 20 min. To conduct experiments that used PCAs to investigate the molecular interaction of the SR-BI and SIPR1 receptors, 0.3 μg of Venus-1-tagged SR-BI were transiently cotransfected in combination with either 0.3 μg of Venus-2 or Venus-1-tagged S1PR1 DNAs into HEK293 cells cultured in serum-free medium using FuGene HD. Eighteen hours after transfection, cells were stimulated with agonists for 20 min. Cells were fixed with 4% formaldehyde/PBS and washed with ice-cold PBS. Confocal microscopy was performed using a Zeiss LSM 510 META laser scanning microscope (Carl Zeiss, Inc., Thornwood, NY) equipped with a 60× objective using excitation at 488 nm and emission at 505–530 nm for GFP fluorescent and excitation at 543 nm and emission at 560–615 nm for mCherry fluorescent wavelengths.

Silencing of SR-BI

HEK293 cells were plated onto 6-well plates and grown to 50–70% confluence at least 24 h before siRNA transfection. The transfection reagent (8 μl) (OriGene, Rockville, MD) was diluted with serum-free MEM (40 μl), and RNA mixtures containing 20 nM siRNA, 30 μl siRNA diluent, and 15 μl serum-free MEM were prepared. Both solutions were allowed to stand for 5 min at room temperature and then combined and mixed by inversion. The mixture was allowed to stand for an additional 20 min at room temperature and then was added to cultures containing 1 ml of fresh serum-free MEM. Cells were incubated for 4 h at 37°C, and

then an additional 1 ml of MEM containing 20% FBS and 2% penicillin/streptomycin was added to each well. Twenty-four hours after transfection, cells were seeded on collagen-coated, clear-bottomed, black-walled 96-well plates for determination of intracellular calcium level. The efficiency of mRNA downregulation was determined using quantitative real time PCR.

Quantification of SR-BI mRNA levels using real time PCR

SR-BI mRNA abundance was assayed by quantitative real-time PCR using the CFX96 iCycler (Bio-Rad, Hercules, CA) with two primer sequences: SRBI-forward: ATACGTGTACAGGGAGTTC; SRBI-reverse: GGCTTATTCTCCATCATCAC.

Total RNA was isolated from cells using the High Pure RNA Isolation Kit (Roche Diagnostics GmbH, Indianapolis, IN). cDNA was synthesized from each RNA sample (1 µg of total RNA per reaction) using the iScriptcDNA Synthesis Kit (Bio-Rad) by amplifying the reaction one cycle in a GENIUS thermocycler (25°C for 5 min, 42°C for 30 min, 80°C for 5 min). The amplified cDNA was used as a template for quantitative real-time PCR using iQ SYBR Green Supermix (Bio-Rad) according to the manufacturer's instructions. Data were analyzed using the iCycler software (Bio-Rad). Expression of SR-BI mRNA was normalized to the mRNA expression level of the housekeeping gene, GAPDH.

Assessment of S1PR1 receptor internalization

S1PR1-YFP internalization was quantified in live HEK293 cells using the In-Cell 2000 imaging platform (GE Healthcare Bio-Sciences, Piscataway, NJ). YFP and DAPI channel filters were used to image each field at 40× magnification every minute for 20 min to produce an image stack with kinetic data. To conduct an experiment, rHDL+S1P, S1P, HDL2, or HDL3 were acutely added to the assay well at a final concentration of 30 µg/ml for rHDL + S1P, 0.1 µM for S1P, and 500 µg/ml for HDL2 and HDL3. Object formation over time, or vesicle counts, which is indicative of S1PR-YFP internalization, were determined for each imaged cell and then averaged across experimental repeats using DotQuanta. DotQuanta is a commercially available (Wellspring, LLC via Flintbox, https://flintbox.com/public/project/26187/) platform-independent Python-based program that enables users to process and quantitate multiple monochrome live-cell microscopy images. This program localizes fluorescently stained nuclei, segments cells based on deciphering cellular fluorescence expression, and counts the number of "objects," or puncta, formed over time based on pixel aggregation. DotQuanta is derived from the first iteration of the real-time quantitative algorithm previously described (32).

Analysis of physical interaction between HDL receptor SR-BI and S1PR1 using PCA

One day prior to initiation of transfection, HEK293 cells were seeded into 6-well cluster plates to attain 50–70% confluency. To conduct a study, 0.5-µg aliquots of cDNA coding for SRBI-Venus1 and S1PR1-Venus2 for experimental incubations, or cDNA coding for S1PR1-Venus1 or PTH1R-Venus2 in control incubations, were cotransfected into each well. To confirm the specificity of the PCA, additional control cultures were cotransfected with increasing concentrations of cDNA coding for nonconjugated SRBI or with empty plasmid vector. The cultures were incubated 24 h after the transfection, after which the culture medium was removed and the cultures washed using PBS. The cultures were then incubated an additional 6 h with serum-free medium, after which the cells were detached from the plate, centrifuged, and suspended in HBSS supplemented with 25 mM HEPES (pH 7.4). Equal volume aliquots of cells were transferred to four 1.5 ml Eppendorf tubes, and HDL2, HDL3, or S1P were added to each tube

at the indicated concentrations. The tubes were incubated 30 min in a CO_2 incubator. After the incubation, to minimize HDL-mediated autofluorescence, the cell suspensions were again centrifuged, the supernatant was decanted, and the cells were resuspended in 320 µl of BRET buffer (1 mM $CaCl_2$, 140 mM NaCl, 2.7 mM KCl, 900 mM $MgCl_2$, 370 mM NaH_2PO_4, 5.5 mM d-glucose, 12 mM $NaHCO_3$, 25 mM HEPES; pH 7.4), and a 100 µl aliquot of each cell suspension was inoculated into each well in black-wall, clear bottomed, 96-well cluster plates for analysis. Background and cellular YFP fluorescence were quantitated using a SpectraMaxRi3× microplate reader (Molecular Devices) with 488 nm excitation and 535 emission filters. YFP fluorescence generated in cells incubated with HDL3 or S1P was calculated after subtracting fluorescence levels developed in control incubations in the same experiment using cells incubated only with BRET buffer.

RESULTS

HDL-mediated intracellular calcium levels in RVSM and HEK293 cells

It has been shown previously that HDL increases intracellular calcium concentration in various cell types (1, 10, 14, 33, 34). S1P also has been shown to regulate calcium mobilization that was sensitive to pertussis toxin (35, 36), suggesting the involvement of G protein-coupled S1P receptors. However, the potential role of S1P contained in the regulation of intracellular calcium level is not well defined. To investigate S1P involvement in HDL-mediated intracellular calcium mobilization, RVSM and HEK293 cells were incubated with rHDL particles formulated with or without S1P or with increasing concentrations of HDL2, HDL3, or S1P, and the influx of intracellular calcium level was determined using a FLIPR^{TETRA} instrument (Molecular Devices). Intracellular calcium influx was substantially increased when cells were incubated with rHDL particles supplemented with S1P (rHDL + S1P) but not when the cells were incubated with rHDL without S1P supplementation (rHDL) (**Fig. 1A**). This strongly suggests that S1P in rHDL is responsible for the majority of HDL-mediated intracellular calcium release in RVSM and HEK293 cells. In addition, intracellular calcium concentrations were increased in a dose-dependent manner in cells incubated with HDL2 (Fig. 1B), HDL3 (Fig. 1C), and S1P (Fig. 1D) in both cell types. These data further suggest that S1P in HDL can mediate intracellular calcium release in RVSM and HEK293 cells.

Internalization of S1PR1 in response to HDL stimulation

A characteristic feature of most G-coupled receptors is ligand-dependent internalization (37). We have previously shown that insulin-like growth factors activate S1PR1 by stimulating sphingosine kinase 1, leading to increased intracellular and extracellular S1P concentration (23). Because S1PR1 internalization is activation dependent, it can be used as a marker of receptor activity (23). To determine the effect of S1P transported in HDL on the activation of cellular S1P receptors, we used confocal microscopy to monitor the internalization of GFP-tagged S1PR1 receptor,
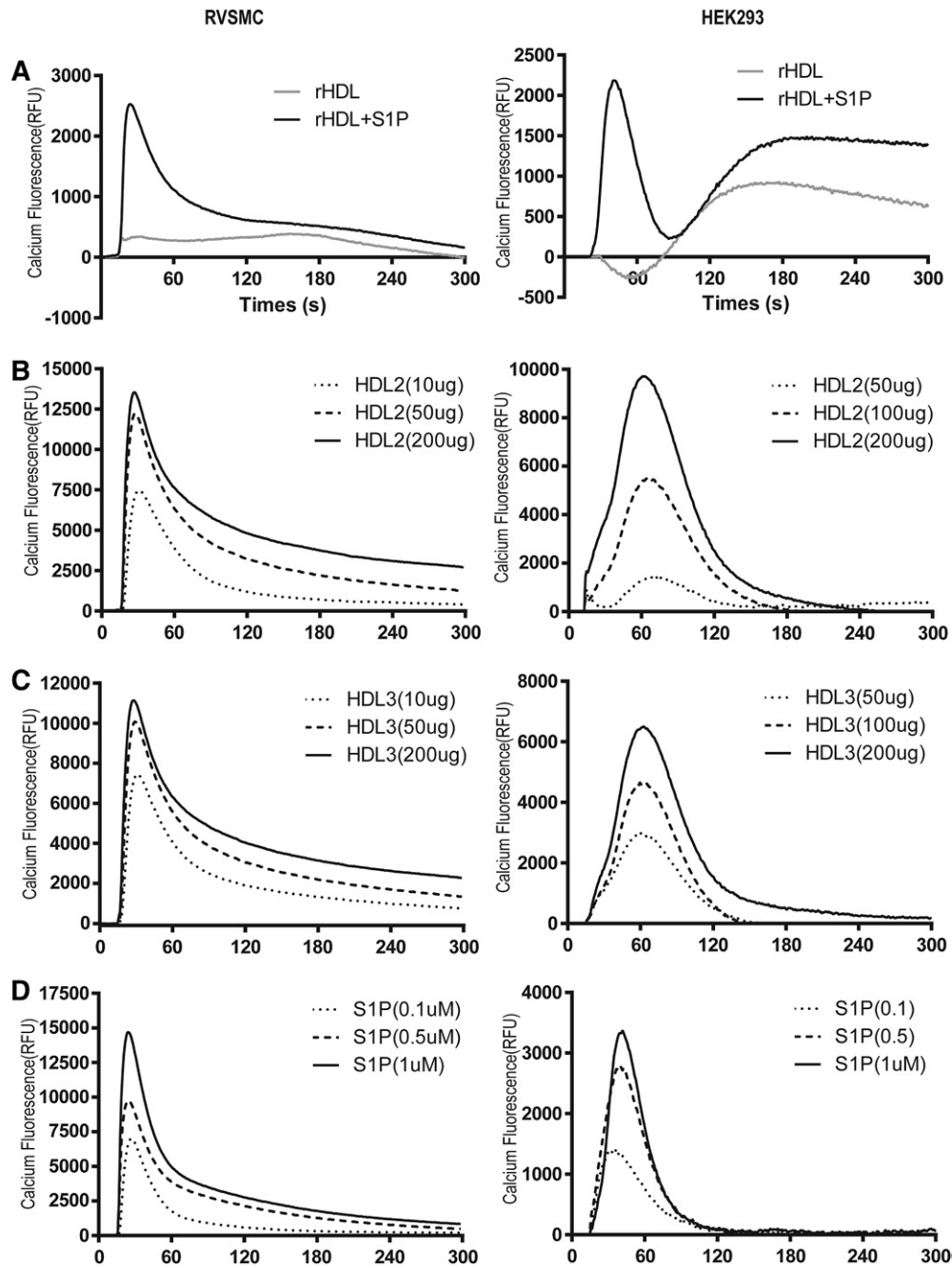
Fig. 1. Time course of intracellular calcium influx in RVSM cells (RVSMC) and HEK293 cells incubated with rHDL or rHDL + S1P (A), HDL2 (B), HDL3 (C), and molecular S1P (D). Assay and ligand dosing plates were loaded into *FLIPR*[TETRA], and fluorescence intensity was recorded every 1 s for 10 reads to establish baseline fluorescence and then every 1 s for 300 reads (310 total reads over 5.17 min). Raw data representing the time-fluorescence relationship for each well after ligand addition were exported to Microsoft Excel for subtraction of background fluorescence and data analysis. The final concentrations in each well for each agonist are rHDL and rHDL + S1P (30 µg protein/ml), HDL2 and HDL3 (10, 50, and 200 µg/ml) in RVSM cells and (50, 200, and 500 µg/ml) in HEK293, and S1P (0.1, 0.5, and 1 µM). The final concentration of S1P in the culture medium for cells incubated with rHDL + S1P was set at 120 µM as was used in our previous studies (16) to approximate S1P levels in HDL (15). For clarity, only data collected at even-numbered time points are plotted. The calcium ionophore A23187 (10 µM) was used in each experiment as the positive control. Data shown are the average fluorescence intensities obtained in five independent experiments.

which had been transfected into HEK293 cells as a biological sensor for activation of the receptor. Upon exposure to S1P, GFP-S1PR1 receptors expressed in HEK293 cells underwent striking rearrangement from a uniform distribution on the plasma membrane (NS: nonstimulated, basal conditions) to a punctate distribution within the cell cytoplasm, consistent with activation-dependent receptor internalization (Fig. 2A). Treatment with HDL2 and HDL3 produced a

similar pattern of receptor distribution, suggesting that incubation of the cells with HDL induced activation of S1P receptors. To test whether this activation of the S1PR1 receptors resulted specifically from S1P contained in the HDL particles, the experiments were repeated using rHDL with and without S1P. Only rHDL with S1P incorporated into the particle, but not rHDL alone, activated S1PR1, suggesting that S1P in HDL was the major activator for S1PR1 internalization (**Fig. 2A**). To monitor S1PR trafficking, HEK293 cells transfected with the gene coding for YFP-tagged S1PR1 receptor protein were stimulated with rHDL+S1P, HDL2, HDL3, or S1P, and localization of the receptor protein was monitored using time-resolved fluorescent microscopy coupled with semiautomated, high-content, multiparametric analysis. We quantified trafficking of the receptors every minute for 20 min (Fig. 2B). When cells were stimulated by rHDL+S1P, HDL2, and HDL3, the number of internalized vesicles of S1PR1 gradually increased over time and began to plateau only after approximately 15 min. However, when cells were stimulated using molecular S1P not transported by a lipoprotein, the number of internalized vesicles of S1PR1 increased more rapidly and plateaued by approximately 10 min after initiation of stimulation. The slower rate of internalization of the

S1PR receptors after incubating the cells with HDL suggests a more complex activation process involving movement of the S1P molecule out of HDL and its subsequent binding to cellular S1PR to enable S1PR activation and internalization.

Inhibition of HDL-mediated increase in intracellular calcium concentration by S1PR1, S1PR2, and S1PR3 antagonists and the Gi inhibitor PTX in RVSM and HEK293 cells

S1P transported by rHDL (rHDL + S1P), but not rHDL itself, increased intracellular calcium levels in RVSM and HEK293 cells (Fig. 1A). To determine whether S1P receptors are involved in HDL-mediated intracellular calcium mobilization, maximum intracellular calcium influx was measured in the presence of the Gi inhibitor PTX, the S1PR1 and S1PR3 antagonist VPC23019, and the S1PR2 antagonist JTE-013. The maximum calcium signals observed release when cells were incubated with HDL2, HDL3, or S1P were normalized to the maximum observed without any inhibitor present. The maximal intracellular calcium concentrations in RVSM or HEK293 cells incubated with HDL or S1P were inhibited by PTX about by 40–60% in RVSM (**Fig. 3A**) and HEK293 cells (Fig. 3B). In
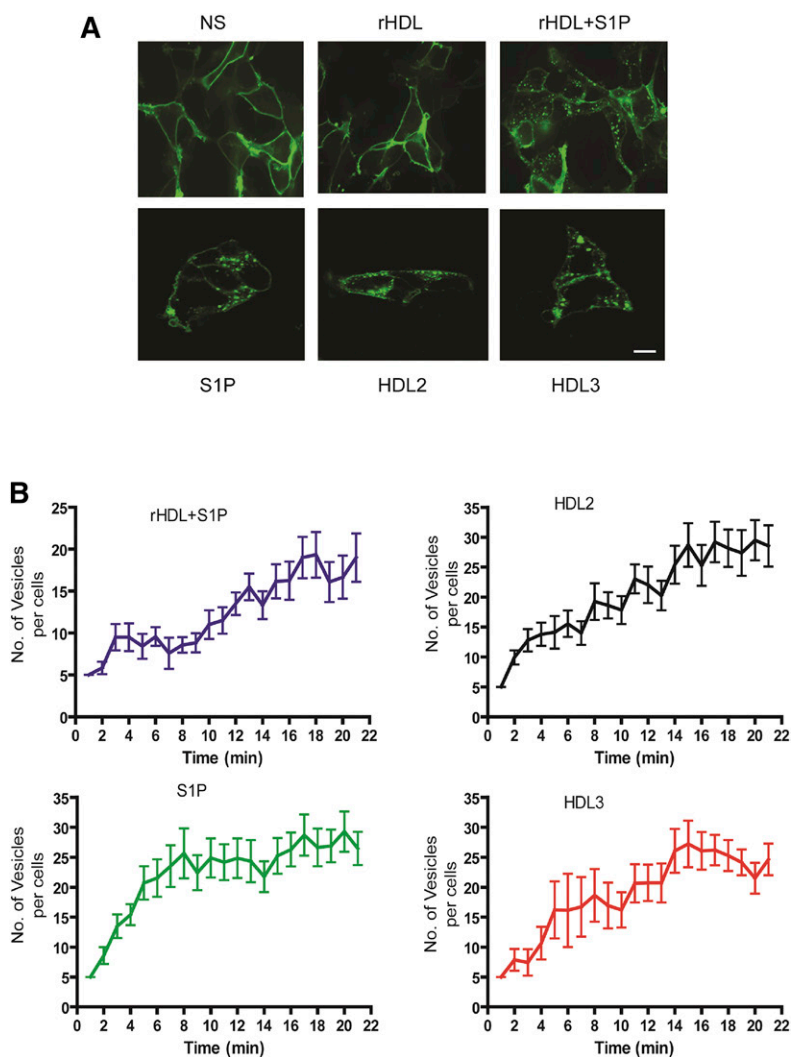

Fig. 2. Cellular distribution of GFP-tagged S1PR1 in HEK293 cells incubated with rHDL, rHDL + S1P, HDL2, HDL3, or S1P (A) and the time course of the trafficking of vesicles containing GFP-tagged S1PR1 in HEK293 cells (B). A: HEK293 cells were transiently transfected with cDNA coding for GFP-tagged S1PR1 protein. The cells were serum deprived and then incubated with the indicated ligand at the following final concentration in the media: rHDL or rHDL + S1P (30 µg protein/ml), HDL2 or HDL3 (500 µg/ml), or S1P (0.1 µM). Cells were incubated with each ligand for 15 min prior to fixation and subsequent determination of the cellular distribution of GFP-S1PR1 using confocal microscopy. Images shown are representative confocal fields from one of three independent experiments that gave similar results. Bar in the HDL3 panel indicates 10 µm and applies to all other images in panel. B: To analyze the time course of the mobilization of S1PR1 in live cells, cDNA coding for the YFP-tagged S1PR1 receptor was transfected into HEK293 cells, and the cells were incubated with the ligands at the following final concentrations: rHDL + S1P (30 µg/ml), HDL2 or HDL3 (500 µg/ml), or S1P (0.1 µM). Fluorescence intensity on a per-cell basis was collected over a course of 20 min using the IN Cell imaging platform. Object formation over time, or vesicle counts, which are indicative of S1PR-YFP internalization, were determined for each imaged cell and then averaged across multiple experimental repeats using DotQuanta software. Data shown are the average of S1P-YFP vesicles internalized per cell for each of three independent experiments. There was no time-dependent increase in fluorescence in control cells with no addition to the culture medium (NS) or in cells incubated with rHDL.
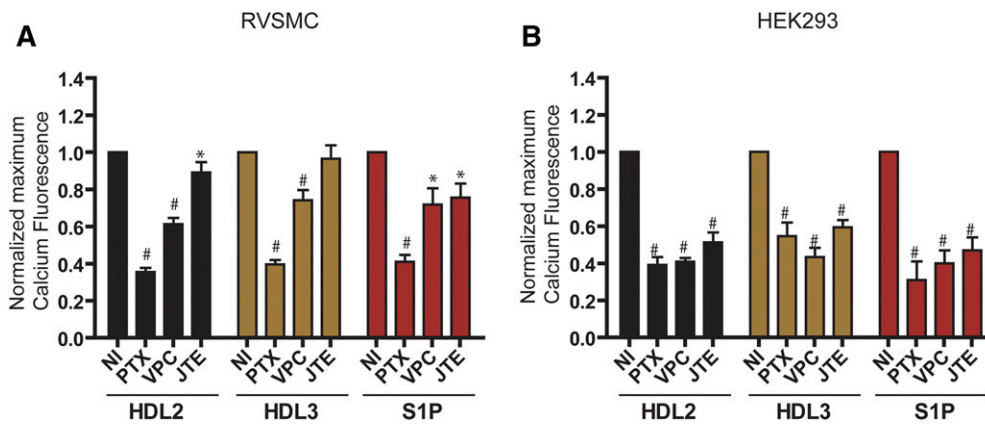
Fig. 3. The effects of Gi/o inhibitor, PTX, and of the competitive S1PR1 and S1PR3, S1PR2 receptor antagonists VPC23019 and JTE-013 on HDL2-, HDL3-, and S1P-stimulated maximum intracellular calcium influx in RVSM cells (RVMSC) (A) and HEK293 (B) cells. Serum-deprived RVSM and HEK293 cells were pretreated overnight with 0.7 ng/ml PTX or with 10 µM VPC23019 or 10 µM JTE-013 for 1 h before loading the calcium-sensitive dye. Cells were then incubated for 1 h at 37°C, 5% CO_2. Determinations of cellular calcium influx were conducted at room temperature using the FLIPR^{TETRA} instrument. Bar graphs represent mean ± SE of five independent experiments. The maximum calcium levels obtained from inhibitor-treated cells incubated with HDL2, HDL3, or S1P are normalized to the maximum calcium level measured in untreated cells. NI, no inhibitor. * $P < 0.05$, # $P < 0.005$ versus NI.

RVSM cells, the maximal rates of intracellular calcium release in cells incubated with HDL or S1P were significantly reduced by VPC23019 but were relatively unaffected after incubation with JTE-013. However, the HDL- and S1P-mediated maximum rates of calcium release were significantly decreased in the presence of both VPC23019 and JTE-013 in HEK293 cells. These data strongly suggest that in RVSM and HEK293 cells, cellular Gi/0-coupled S1P receptors mediate the intracellular calcium signal that results from the metabolism of HDL-bound S1P.

The role SR-BI on HDL-mediated increase in intracellular calcium levels in HEK293 cells

G protein-coupled S1P receptors are involved in HDL-mediated intracellular calcium flux in RVSM and HEK293 cells (Fig. 3). It has been established that SR-BI is a functional receptor for native HDL particles that mediates selective lipid uptake from lipoprotein particles and efflux of unesterified cholesterol from cells to lipoprotein particles (1, 3). Furthermore, SR-BI is involved in HDL signal transduction (38–42). To determine if SR-BI is involved in HDL-mediated intracellular calcium mobilization, we used siRNA-silencing to downregulate SR-BI gene expression and determined the maximum intracellular calcium signal with and without SR-BI gene downregulation. Using three different, target-specific siRNAs to downregulate SR-BI gene expression, we were able to reduce the expression of the SR-BI gene approximately 71% in HEK293 cells (**Fig. 4A**). We transfected HEK293 cells with control siRNAs compared with siSR-BI using the same transfection protocol and determined the maximum intracellular calcium responses after stimulation of cells with HDL2, HDL3, or S1P. Downregulation of SR-BI expression reduced the maximum intracellular calcium concentrations 51% to 56% in cells incubated with HDL2 or HDL3, whereas the

maximum intracellular calcium concentrations were unaffected in cells incubated with S1P (Fig. 4B), suggesting that SR-BI is at least partially involved in HDL2- and HDL3-mediated intracellular calcium flux in HEK293 cells. The participation of alternative HDL binding receptors in HDL-mediated intracellular calcium response in HEK293 remains to be determined.

Interaction between SR-BI and S1PR1

We have shown thus far that S1P receptors are required to affect intracellular calcium flux in RVSM and HEK293 cells that have been stimulated by S1P transported by HDL (Fig. 3) and that the SR-BI receptor also is involved in HDL-mediated intracellular calcium release in HEK293 cells (Fig. 4). We have shown previously that HDL-mediated plasminogen activator inhibitor-1 secretion requires SR-BI and S1PR2 in 3T3L1 cells (16). It has been suggested that the binding of HDL to the SR-BI receptor could provide the necessary spatial proximity for HDL-bound S1P to effectively stimulate S1P receptors such that SR-BI is the docking receptor that captures HDL particles to facilitate the release of S1P to activate cellular S1P receptors (14, 20). However, no previous studies have investigated the physical interaction between cell surface SR-BI and S1PRs when cells are stimulated with HDL. Therefore, we explored the molecular interaction between SR-BI and S1P receptors In HEK293 cells stimulated with HDL.

We first investigated the spatial distributions of the SR-BI and S1PR1 receptors in cell membranes using HEK293 cells transfected with plasmids coding for the GFP-SR-BI and mCherry S1PR1 receptor proteins. In control incubations without any additions to the media (NS), SR-BI receptors were primarily localized on the plasma membrane and within a few intracellular puncta (**Fig. 5**). Consistent with this, previous studies in Chinese hamster ovary cells transiently
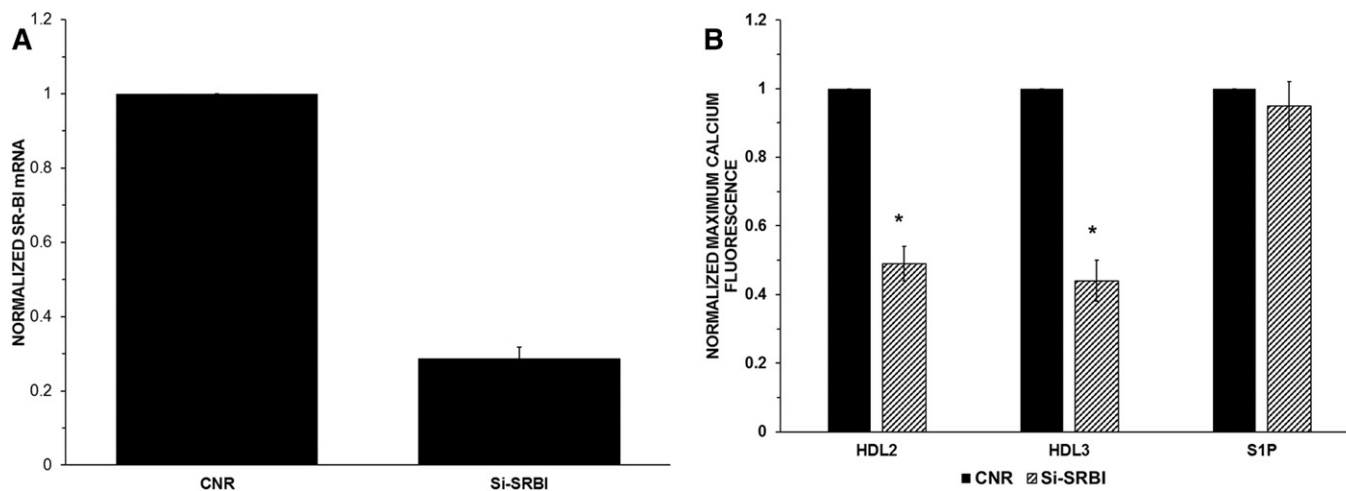
Fig. 4. Determination of the role of SR-BI in HDL2-, HDL3-, and S1P-mediated maximum intracellular calcium influx in HEK293 cells. HEK293 cells were transiently transfected with 20 nM of siRNA to downregulate the expression of the gene coding for SR-BI. Twenty-four hours after transfection, the cells were seeded onto collagen-coated, clear-bottomed, black-wall 96-well plates. At 48–72 h after each transient transfection, the assay of intracellular calcium efflux was conducted using the FLIPR[TETRA] instrument. A: Relative expression of the gene coding for SR-BI in HEK293 incubated with control siRNA (CNR) or siRNA targeted to SR-BI. B: The maximum calcium signals obtained in HEK293 cells treated with siSR-BI were normalized to the maximum calcium level determined in cells treated with control siRNA (CNR) when the cells were exposed to HDL2 or HDL3 (500 µg/ml) or S1P (0.1 µM). * $P < 0.05$ versus CNR in incubations with the same lipoprotein. Data shown are the mean ± SE of four independent experiments.

transfected with GFP-tagged SR-BI fusion proteins reported that approximately 70% of the SR-BI protein was localized on the plasma membrane in patches and in small extensions of the cell surface, and 30–40% the protein was intracellular (43, 44). Likewise, S1PR1 was localized only on the cell plasma membrane in unstimulated cells (Fig. 5A). After incubation with HDL or S1P, S1PR1 receptor fluorescence adopted a punctuate distribution within endosomal vesicles, whereas SR-BI receptor fluorescence remained localized mainly in the plasma membrane (Fig. 5A). This is consistent with the known metabolism of SR-BI, which does not undergo constitutive recycling or cargo-dependent internalization (43). Although both SR-BI and S1PR1 were localized initially on the plasma membrane, there was no colocalization of these two proteins when the cells were incubated with HDL3 or S1P (Fig. 5A).

To further investigate the cellular trafficking of the SR-BI and S1PR1 proteins, we conducted similar experiments with living cells and rigorously quantitated the temporal formation of vesicles containing SRBI-GFP and S1PR1-mCherry proteins in cells using the IN-Cell imaging platform (Fig. 5B–D). The incubation of HEK293 cells with HDL3 or S1P stimulated a significant increase (>5-fold) in the number of vesicles containing S1PR1-Cherry or SR-BI-GFP (Fig. 5B and C, respectively), with only a modest increase in the number of vesicles containing both SRBI-GFP and S1P-Cherry after stimulation with HDL3 or S1P (Fig. 5D). This observation is in agreement with the results of our previous studies using fixed cells (Fig. 5A) and suggests that, once activated by S1P delivered by SR-B1-bound HDL, S1PR1 traffics independently from SR-B1.

We next tested the hypothesis that SR-B1 and S1PR1 physically interact on the plasma membrane during delivery of S1P from the HDL particle to S1PRs. PCAs are used

to identify protein-protein interactions in biological systems (45). The proteins of interest (SR-BI and S1PR1) were prepared as chimeric proteins, each fused to an incomplete fragment of a third "reporter" protein. In this study, we used YFP as the reporter protein such that the two split versions of the YFP protein, Venus1 (bait) and Venus2 (prey), were fused to the intracellular C termini of the SR-BI and S1PR1 receptors, respectively (**Fig. 6A**). Only close proximity between the SR-BI and S1PR1 receptor proteins will bring the Venus1 and Venus2 fragments of YFP into sufficient proximity that YFP can reform a native, 3D structure that can emit a fluorescent signal. This fluorescent signal can be detected, quantitated, and ultimately localized within a cell. The plasmid DNAs coding for SR-BI-Venus1 and S1PR1-Venus1 or S1PR2-Venus2 were transiently cotransfected into HEK293 cells. When the cells were transfected with the plasmid DNAs coding for the complementary portions of the reporter protein (SR-BI-Venus1 and S1PR1-Venus2), HDL3 stimulated the molecular interaction between the S1PR1 and SR-BI receptors and resulted in a significant increase in fluorescence level in the cell (Fig. 6B). Most importantly, when cells were incubated with molecular S1P, which does not interact with or require the SR-BI receptor to alter cell metabolism, there was no increase in cellular fluorescence, indicating that molecular S1P did not stimulate the interaction between the SR-BI and S1PR1 receptors (Fig. 6C). Thus, these studies suggest that when cells were incubated with HDL3, the SR-BI and S1PR1 receptors moved closer and came together at the molecular level to enable the two complementary interacting proteins, Venus1 and Venus2, to fuse and ultimately produce a significant increase in the fluorescence signal in the cell. To validate the PCA, we conducted three series of control studies. In the first series of control incubations,
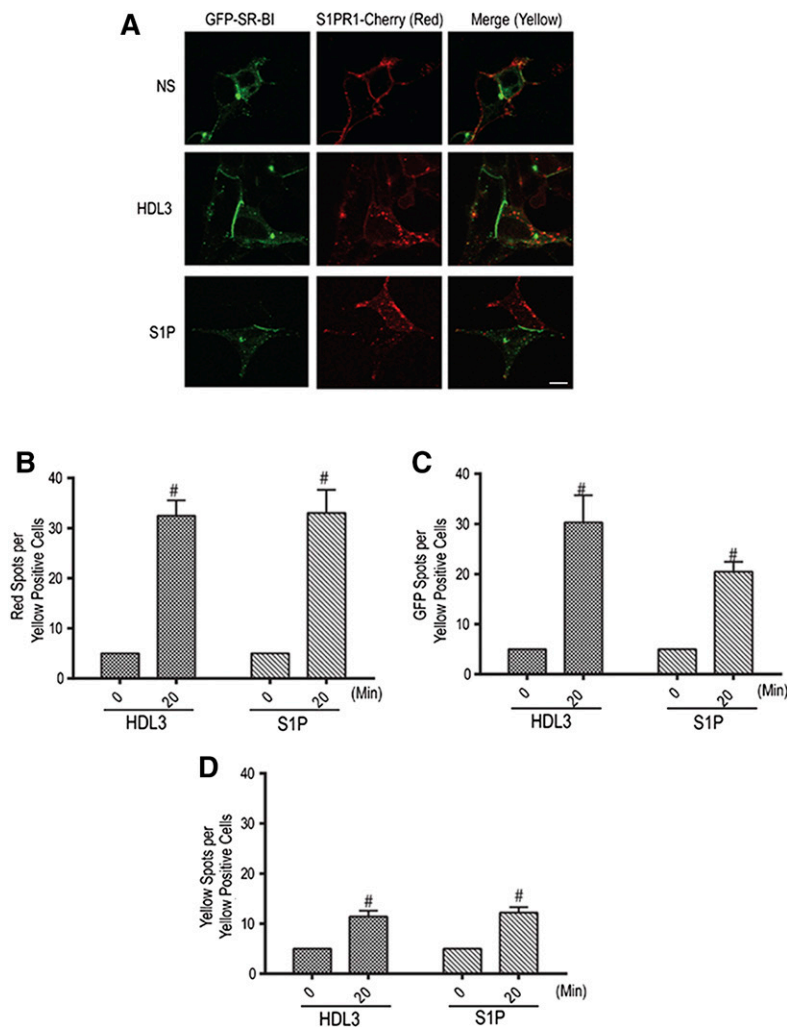
Fig. 5. Distribution of GFP-tagged SR-BI and mCherry-tagged S1PR1 receptor proteins in fixed HEK293 cells (A) and their trafficking patterns in live cells (B–D). A: HEK293 cells were transiently cotransfected with cDNA coding for the GFP-tagged SR-BI and mCherry-tagged S1PR1 receptor proteins. Serum-deprived cells were incubated with HDL3 (500 µg/ml) or S1P (0.1 µM) for 20 min before fixation and determination of the cellular distribution of GFP-SR-BI and S1PR1-Cherry fluorescence using confocal microscopy. B–D: The same experiment as described in (A) was carried out in live HEK293 cells using the GE IN Cell imaging platform to quantitate the number of vesicles transporting SRBI-GFP and S1PR1-Cherry proteins at baseline and after incubating for 20 min. B: The time course of the formation of vesicles containing mCherry-S1PR1 in cells incubated with HDL3 or S1P. C: The time course of the formation of vesicles containing GFP-SR-BI in cells incubated with HDL3 or S1P. D: The time course of the formation of vesicles containing both SRBI-GFP and S1P-Cherry (double spot vesicle) after incubating the cells with HDL3 or S1P. Vesicles formed in each cell were counted every 30 s for 20 min after cells were stimulated with HDL3 or S1P using real-time fluorescence microscopy. Each bar graphs represents the mean ± SE of three independent experiments. [#] $P < 0.005$ versus time = 0.

HEK293 cells were cotransfected with plasmid DNAs encoding the two noncomplementary parts of the reporter protein (i.e., SR-BI-Venus1 and S1PR1-Venus1). There was no detectable increase in the levels of cellular fluorescence when the cells were incubated with either HDL3 or S1P, supporting the specificity of the PCA (Fig. 6C). In the second series of control incubations, HEK293 cells were again cotransfected with cDNA coding for the complementary portions of the reporter protein (SR-BI-Venus1 and S1PR1-Venus2). In the same experiment, companion cultures were cotransfected with cDNA coding for the complementary portions of the reporter protein (SR-BI-Venus1 and PTH1R1-Venus2), and the cultures were incubated with HDL3 or molecular S1P. There was a significant increase in cellular fluorescence in the cultures transfected with cDNA coding for SR-BI-Venus1 and S1PR1-Venus2 when the cells were incubated with HDL3 but not with molecular S1P, again supporting the hypothesis that when cells are incubated with HDL3, the SR-BI and S1PR1 receptors move into close proximity and come together at the molecular level. In contrast, when cultures were transfected with cDNA coding for SR-BI-Venus1 and PTH1R1-Venus2, proteins that do not interact in the cell membrane, neither HDL3 nor S1P added to the culture medium altered cell fluorescence levels, supporting the hypothesis that the

SR-BI and PTH1R1 proteins do not interact at the molecular level and further confirming the specificity of the PCA (Fig. 6D). In the third series of control experiments, HEK293 cells were cotransfected with cDNA coding for the complementary portions of the reporter protein (SR-BI-Venus1 and S1PR1-Venus2) together with increasing amounts of cDNA coding for nonconjugated SR-BI protein. The expression of increasing amounts of nonconjugated SR-BI protein should compete with the conjugated SR-BI protein for interaction with conjugated S1PR1 to reduce the PCA response. Transfection of cells with increasing amounts of cDNA coding for competing, nonconjugated SR-BI protein significantly decreased the PCA response in cultures incubated with HDL3, confirming the specificity of the PCA (Fig. 6E).

We conducted additional experiments to determine the cellular location where S1PR1 interacted with the SR-BI receptor during stimulation with HDL3 by repeating the same experiments using confocal microscopy to localize the fluorescence signal. When cells were incubated in control conditions without any addition to the medium (NS), the fluorescence signal (indicating the molecular interaction of the S1PR1 and SR-BI receptors) was weak and spread diffusely throughout the cell, consistent with random complementation of the Venus1 and Venus2 fragments
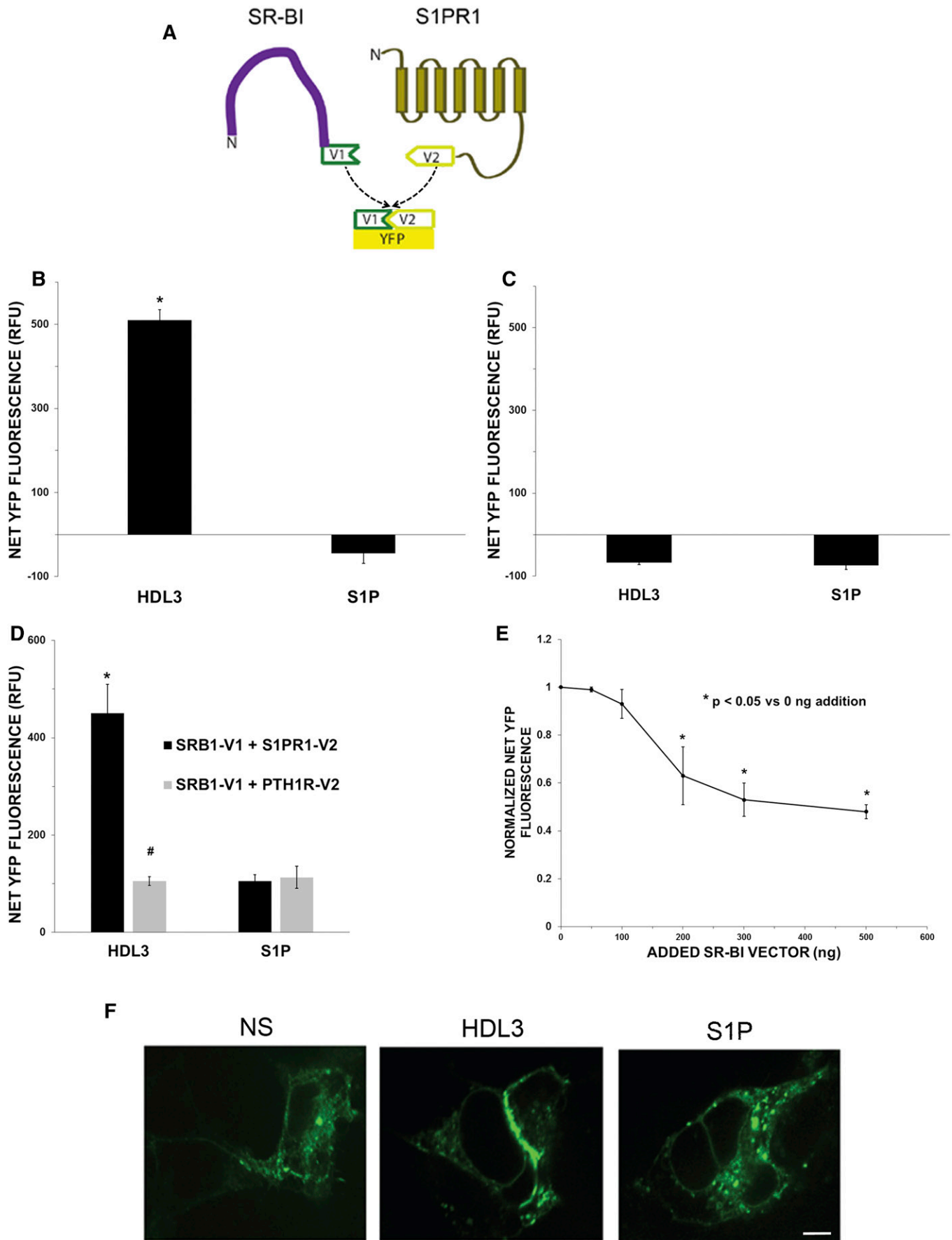
(Fig. 6F). In striking contrast, when cells were stimulated with HDL3, the YFP fluorescence signal specifically increased on the plasma membrane, suggesting that HDL binding to SR-BI promotes its association with S1PR1. In agreement with the results presented in Fig. 6B and D, there was no significant increase in plasma membrane YFP fluorescence when the cells were incubated with molecular S1P, suggesting that direct delivery of S1P did not stimulate the molecular interaction between the SR-BI and S1PR1 receptors.

DISCUSSION

We have shown that S1P transported in HDL is biologically active and is a major effector of HDL-mediated increase in intracellular calcium. We have also shown that the S1PR1 and S1PR3 receptors mediate calcium mobilization in the RVSM and HEK293 cells stimulated with HDL. Furthermore, SR-BI, a major HDL binding receptor, was required for intracellular calcium release in these cells. We provide strong evidence, using protein fragment complementation, that the S1PR1 and SR-BI receptors interact at the molecular level to affect HDL-associated S1P changes to cell metabolism.

Previous studies have shown that SR-BI is localized in punctate microdomains across the surface and on the edges of cells (46). We investigated the cellular movement of SR-BI receptors using confocal microscopy to track the fluorescence emanating from SR-BI receptors conjugated to GFP and showed that SR-BI was localized in patches and in small extensions of the cell surface. Previous investigations used electron microscopy to demonstrate that the SR-BI receptor was localized in patches or clusters primarily on microvillar extensions of the plasma membrane (44).

In 3T3-L1 adipocytes, SR-BI was mainly distributed in the cytoplasm, and insulin, angiotensin, and HDL stimulation led to recruitment of SR-BI to the cell surface (47). However, the results of other studies were inconsistent and demonstrated variable subcellular localization of the SR-BI receptor in different tissues, suggesting the potential for a dynamic movement of the SR-BI receptor in the cell. In our study, we found that the SR-BI protein was localized primarily on the plasma membrane with some protein extending into the cytoplasm, in agreement with data reported previously (43, 44). Based on our data gained using fluorescence confocal microscopy, HDL incubated with cells did not result in a significant redistribution of SR-BI in HEK293 cells, but incubation with HDL did stimulate increased internalization of YFP-tagged or mCherry-tagged S1PR1 (Figs. 2 and 5). Furthermore, incubation of cells with S1P in HDL (HDL-S1P) compared with molecular S1P resulted in a different trafficking pattern for S1PR1. Incubation of cells with molecular S1P induced faster internalization of S1PR1 compared with that when cells were incubated with rHDL+S1p, HDL2, and HDL3 (Fig. 5). We also clearly demonstrated that it is S1P in the HDL particle that is the major HDL constituent to activate the S1PR1 receptor (Fig. 2).

Previous studies have suggested that many changes in cell function mediated by HDL require the activity of the SR-BI and/or S1P receptors individually or in concert (14, 17, 18, 20). These observations have led to the hypothesis that the binding of HDL to the SR-B1 receptor may provide the necessary spatial geometry to bring HDL-S1P sufficiently close to its cognate receptors to initiate the various S1PR-mediated signaling cascades (20, 22). We conducted two different experimental approaches to investigate the result of incubating cells with HDL-S1P or molecular S1P on altering the molecular distribution of the SR-BI and S1PR1

Fig. 6. PCA of bimolecular fluorescence resulting from the molecular interaction between SR-BI and S1PR1. A: The proteins of interest (SR-BI and S1PR1) were each covalently linked to an incomplete fragment of the "reporter" protein YFP such that the two split versions of the YFP protein, Venus1 (V1, bait) and Venus2 (V2, prey), were conjugated to the SR-BI and S1PR1 receptors, respectively. The molecular interaction between SR-BI and S1PR1 will bring together Venus1 and Venus2 to form functional YFP. B: HEK293 cells were transiently cotransfected with cDNA coding for SR-BI-Venus1 and S1PR1-Venus2 to quantitate the interaction between the SR-BI and S1PR1 receptor proteins in cells without any addition to the medium or in cells incubated with HDL3, in which S1P is transported at high concentrations, or with molecular S1P added to the medium. HDL3 stimulates the molecular interaction between the SR-BI and S1PR1 receptor proteins to bring the fragments of the YFP reporter protein within sufficiently close proximity to allow YFP to reform its native, 3D structure and emit a fluorescent signal. Molecular S1P does not require binding to SR-BI and does not stimulate the interaction between the SR-BI and SiPR1 receptors and thus does not increase the fluorescence signal. C: Fluorescence in cells transiently cotransfected with cDNA coding for the SR-BI-Venus1 and S1PR1-Venus1 proteins, which are noncomplementary and cannot form native YFP, to serve as a negative control. D: Cellular fluorescence in control incubations of HEK293 cells transiently cotransfected with cDNA coding for SR-BI-Venus1 and S1PR1-Venus2 to quantitate the interaction between the SR-BI and S1PR1 receptor proteins or with cDNA coding for SR-BI-Venus1 and PTH1R-Venus2, which do not interact. To evaluate the molecular interaction between the SR-BI and S1PR1 proteins, serum-deprived cells were stimulated with HDL3 or S1P for 20–30 min, and the net change in fluorescence intensity was determined in cells incubated with HDL3 or S1P after subtracting the background fluorescence level. Data are expressed as the net increase in fluorescence in cells incubated with HDL3 or S1P relative to the fluorescence in cells without any addition to the medium. * $P < 0.05$ for incubations with HDL3 versus S1P. # $P < 0.05$ for cells transfected with SR-BI-Venus1 and S1PR1-Venus2 versus SR-BI-Venus1 and PTH1R-Venus2. E: Cellular fluorescence in control incubations of HEK293 cells transfected with SR-BI-Venus1 (500 ng) and S1PR1-Venus2 (500 ng) and with the indicated amount of additional cDNA coding for nonconjugated SR-B1. Cellular fluorescence is normalized to the level of fluorescence developed in cells transfected with similar amounts of SR-BI-Venus1 and S1PR1-Venus2 plus an amount of empty vector equal to the concentration of cDNA coding for nonconjugated SR-BI. * $P < 0.05$ for fluorescence in cells transfected with the indicated amount of cDNA coding for nonconjugated SR-BI versus no additional cDNA. Data in panels B–D are expressed as mean ± SE of five independent experiments. F: Determination of the specific cellular location of the molecular interaction between S1PR1 and SR-BI receptors during stimulation with HDL3 or S1P using confocal microscopy to detect the specific cellular location of the fluorescence signal developed using PCA. Bar in micrograph (S1P addition) indicates 10 µm and applies to all other images in the panel. RFU, relative fluorescence units.

proteins in the cell. In the initial studies, we monitored the distribution of fluorescently tagged SR-BI and S1PR1 receptors proteins transfected into HEK293 cells. The data obtained using this approach showed that, in nonstimulated cells (basal conditions), SR-BI and S1PR1 were colocalized in small extensions of the same space in plasma membranes (Fig. 5A). We also found a very small number of colocalized vesicles in response to HDL3 and S1P stimulation in live cells (Fig. 5C). Stimulation with either HDL or S1P led to a significantly increased internalization of S1R1 (Figs. 2B and 5B). Based on images captured using live cells in HEK293 cells, we found that SR-BI and S1PR1 densely but transiently colocalized within regions of cell membrane, such as lamellipodia and the junction between two cells, after cells were incubated with HDL3 but not after incubating with S1P alone. This suggests the interaction between the SR-BI and S1PR1 receptor proteins may occur transiently after which they dissociate, allowing S1PRs to undergo independent endosomal trafficking.

To study the interaction between two proteins with potentially transient interaction, two segments of YFP (YFP-V1 and YFP-V2) were conjugated to the SR-BI and S1PR1 receptor proteins, and PCA was performed. In this PCA, once the YFP-V1 and YFP-V2 moieties interact, they become covalently linked (and result in production of YFP fluorescence) and never dissociate. Thus, in this assay, the development of fluorescence resulting from the interaction between the YFP-V1 and YFP-V2 can be considered as an estimate of the interaction rate between SR-BI and S1PR1. Incubation of HEK293 cells with S1P-HDL (as HDL3) significantly increased the molecular interaction between the SR-BI and S1PR1 receptor proteins. Incubation of cells with S1P alone failed to increase YFP fluorescence, demonstrating that molecular S1P failed to stimulate the movement of the SR-BI and S1PR1 receptors in the plasma membrane into close proximity. These results clearly show that only HDL-bound S1P (HDL3) stimulates increased interaction between SR-BI and S1PR1.

These data provide direct evidence to support the previously hypothesized physical interactions between the SR-BI and S1PR1 receptor proteins (20, 22, 48, 49). However, additional studies will be required to determine if incubation of other cell types with HDL-S1P stimulates the interaction between these two receptors and whether different interaction rates between SR-BI and the other S1P receptors (S1PR2 and S1PR3) may influence HDL-mediated S1PR signaling and function.

The activation of S1PR by S1P transported in HDL may be more complex and may require the participation of other molecules in addition to SR-BI. Pollard et al. (50) have recently suggested that the extracellular matrix protein procollagen C-endopeptidase enhancer protein 2 interacts with SR-BI and enhances SR-BI-mediated HDL-cholesteryl ester uptake. Whether this interaction has an effect on HDL-associated S1P signaling remains to be determined. Another recent study showed that endothelial lipase also can play an important role in HDL/S1P-mediated vascular responses, endothelial migration, angiogenesis, and activation of S1PR1 and can lead to Akt/endothelial NO synthase

phosphorylation (51). The study hypothesized that HDL hydrolysis by endothelial lipase can release biologically active molecules, including S1P, that may promote the phosphorylation of Akt and endothelial NO synthase in endothelial cells and thereby promote cell migration, tube formation, and angiogenesis. Taken together, these observations suggest that multiple, various mechanisms may be involved in the activation of S1PRs through HDL-S1P-mediated signaling.

ApoM is a reported physiological carrier of S1P on HDL (52). It has been recently suggested that S1P bound to ApoM-containing HDL activates endothelial S1PR1 and results in a suppression of inflammatory responses (53). Although the structure of the ApoM protein supports the binding of S1P and HDL-associated S1P is bound specifically to ApoM such that ApoM-containing HDL contain S1P, whereas HDL devoid of ApoM do not (52), Sattler et al. (54) have clearly demonstrated that S1P can be loaded in vitro or in vivo onto HDL, which are virtually absent of ApoM, and restore the defective signaling of the HDLs. We have shown previously that the S1P content of HDL can be increased significantly after in vitro incubation of the HDL particle with molecular S1P (16) and that this supplemented S1P is biologically active. Because ApoM is present in HDL at a molar concentration significantly greater than that of S1P (55), it is unclear if this exogenous, supplemented S1P is bound selectively to ApoM or is merely bound to the particle in a nonspecific manner. Regardless, the S1P in HDL is biologically active and can modify cell metabolism. Clearly, the role of lipoprotein ApoM in the transfer of S1P in lipoproteins onto cell S1P receptors remains to be determined. It has been further suggested that apoM-containing HDL engage endothelial S1P1 to form a signaling complex with β-arrestin 2 that suppresses nuclear factor κB-dependent inflammatory pathways (53). In another recent study, it was shown that HDL from patients with mild coronary artery disease contains 5-fold less S1P concentration than HDL from healthy individuals (54) and that the S1P-deficient HDL is less efficient in activating endothelial molecular pathways. The study attributed HDL-induced endothelial signaling to the S1P content of the HDL particle. These studies are limited in that the measured signaling outcome is limited to a specific HDL functionality and therefore does not rule out effects of other HDL-associated molecules (e.g., apoA-I).

In conclusion, our studies clearly demonstrate that HDL-associated S1P can stimulate the molecular interaction of the S1PR1 and SR-BI receptor proteins to affect S1P-mediated changes in cell metabolism. We hypothesize further that the presence of other HDL receptors/binding proteins, such as cubilin (56), procollagen C-endopeptidase enhancer protein 2 (50), or others (57), might mediate signaling by HDL-associated S1P at sites where HDL engages these receptors. In addition, it is possible that the interaction between HDL and these additional receptor proteins may selectively and specifically direct HDL-S1P-mediated signaling in a manner that differs distinctly compared with that when S1PRs are activated by S1P in its albumin-bound form.

REFERENCES

1. Nofer, J. R., and M. van Eck. 2011. HDL scavenger receptor class B type I and platelet function. *Curr. Opin. Lipidol.* **22:** 277–282.

2. Krieger, M. 2001. Scavenger receptor class B type I is a multiligand HDL receptor that influences diverse physiologic systems. *J. Clin. Invest.* **108:** 793–797.

3. Saddar, S., C. Mineo, and P. W. Shaul. 2010. Signaling by the high-affinity HDL receptor scavenger receptor B type I. *Arterioscler. Thromb. Vasc. Biol.* **30:** 144–150.

4. Korporaal, S. J., and J. W. Akkerman. 2006. Platelet signaling induced by lipoproteins. *Cardiovasc. Hematol. Agents Med. Chem.* **4:** 93–109.

5. Mineo, C., and P. W. Shaul. 2013. Regulation of signal transduction by HDL. *J. Lipid Res.* **54:** 2315–2324.

6. Tong, X., H. Peng, D. Liu, L. Ji, C. Niu, J. Ren, B. Pan, J. Hu, L. Zheng, and Y. Huang. 2013. High-density lipoprotein of patients with type 2 diabetes mellitus upregulates cyclooxygenase-2 expression and prostacyclin I-2 release in endothelial cells: relationship with HDL-associated sphingosine-1-phosphate. *Cardiovasc. Diabetol.* **12:** 27.

7. Gomaraschi, M., A. Ossoli, S. Pozzi, P. Nilsson, A. B. Cefalu, M. Averna, J. A. Kuivenhoven, G. K. Hovingh, F. Veglia, G. Franceschini, et al. 2014. eNOS activation by HDL is impaired in genetic CETP deficiency. *PLoS One.* **9:** e95925.

8. Calabresi, L., M. Gomaraschi, S. Simonelli, F. Bernini, and G. Franceschini. 2015. HDL and atherosclerosis: Insights from inherited HDL disorders. *Biochim. Biophys. Acta.* **1851:** 13–18.

9. Toth, P. P., and M. H. Davidson. 2010. High-density lipoproteins: marker of cardiovascular risk and therapeutic target. *J. Clin. Lipidol.* **4:** 359–364.

10. Grewal, T., R. Evans, C. Rentero, F. Tebar, L. Cubells, I. de Diego, M. F. Kirchhoff, W. E. Hughes, J. Heeren, K. A. Rye, et al. 2005. Annexin A6 stimulates the membrane recruitment of p120GAP to modulate Ras and Raf-1 activity. *Oncogene.* **24:** 5809–5820.

11. Nofer, J. R., B. Kehrel, M. Fobker, B. Levkau, G. Assmann, and A. von Eckardstein. 2002. HDL and arteriosclerosis: beyond reverse cholesterol transport. *Atherosclerosis.* **161:** 1–16.

12. Nofer, J. R., and G. Assmann. 2005. Atheroprotective effects of high-density lipoprotein-associated lysosphingolipids. *Trends Cardiovasc. Med.* **15:** 265–271.

13. Kimura, T., K. Sato, E. Malchinkhuu, H. Tomura, K. Tamama, A. Kuwabara, M. Murakami, and F. Okajima. 2003. High-density lipoprotein stimulates endothelial cell migration and survival through sphingosine 1-phosphate and its receptors. *Arterioscler. Thromb. Vasc. Biol.* **23:** 1283–1288.

14. Nofer, J. R., M. van der Giet, M. Tolle, I. Wolinska, K. von Wnuck Lipinski, H. A. Baba, U. J. Tietge, A. Godecke, I. Ishii, B. Kleuser, et al. 2004. HDL induces NO-dependent vasorelaxation via the lyso-phospholipid receptor S1P3. *J. Clin. Invest.* **113:** 569–581.

15. Hammad, S. M., J. S. Pierce, F. Soodavar, K. J. Smith, M. M. Al Gadban, B. Rembiesa, R. L. Klein, Y. A. Hannun, J. Bielawski, and A. Bielawska. 2010. Blood sphingolipidomics in healthy humans: impact of sample collection methodology. *J. Lipid Res.* **51:** 3074–3087.

16. Lee, M. H., S. M. Hammad, A. J. Semler, L. M. Luttrell, M. F. Lopes-Virella, and R. L. Klein. 2010. HDL3, but not HDL2, stimulates plasminogen activator inhibitor-1 release from adipocytes: the role of sphingosine-1-phosphate. *J. Lipid Res.* **51:** 2619–2628.

17. Kimura, T., H. Tomura, C. Mogi, A. Kuwabara, A. Damirin, T. Ishizuka, A. Sekiguchi, M. Ishiwara, D. S. Im, K. Sato, et al. 2006. Role of scavenger receptor class B type I and sphingosine 1-phosphate receptors in high density lipoprotein-induced inhibition of adhesion molecule expression in endothelial cells. *J. Biol. Chem.* **281:** 37457–37467.

18. Seetharam, D., C. Mineo, A. K. Gormley, L. L. Gibson, W. Vongpatanasin, K. L. Chambliss, L. D. Hahner, M. L. Cummings, R. L. Kitchens, Y. L. Marcel, et al. 2006. High-density lipoprotein promotes endothelial cell migration and reendothelialization via scavenger receptor-B type I. *Circ. Res.* **98:** 63–72.

19. Argraves, K. M., P. J. Gazzolo, E. M. Groh, B. A. Wilkerson, B. S. Matsuura, W. O. Twal, S. M. Hammad, and W. S. Argraves. 2008. High density lipoprotein-associated sphingosine 1-phosphate promotes endothelial barrier function. *J. Biol. Chem.* **283:** 25074–25081.

20. Okajima, F., K. Sato, and T. Kimura. 2009. Anti-atherogenic actions of high-density lipoprotein through sphingosine 1-phosphate receptors and scavenger receptor class B type I. *Endocr. J.* **56:** 317–334.

21. Kimura, T., H. Tomura, K. Sato, M. Ito, I. Matsuoka, D. S. Im, A. Kuwabara, C. Mogi, H. Itoh, H. Kurose, et al. 2010. Mechanism and role of high density lipoprotein-induced activation of AMP-activated protein kinase in endothelial cells. *J. Biol. Chem.* **285:** 4387–4397.

22. Nofer, J. R. 2008. High-density lipoprotein, sphingosine 1-phosphate, and atherosclerosis. *J. Clin. Lipidol.* **2:** 4–11.

23. El-Shewy, H. M., K. R. Johnson, M. H. Lee, A. A. Jaffa, L. M. Obeid, and L. M. Luttrell. 2006. Insulin-like growth factors mediate hetero-trimeric G protein-dependent ERK1/2 activation by transactivating sphingosine 1-phosphate receptors. *J. Biol. Chem.* **281:** 31399–31407.

24. Bhat, S., M. G. Sorci-Thomas, R. Tuladhar, M. P. Samuel, and M. J. Thomas. 2007. Conformational adaptation of apolipoprotein A-I to discretely sized phospholipid complexes. *Biochemistry.* **46:** 7811–7821.

25. Wilhelm, A. J., Z. M. Owen, J. S. Shah, D. Grayson, J. M. Major, A. S. Bhat, S. Gibbs, D. P. Jr, M. J. Thomas, and M. G. Sorci-Thomas. 2010. Apolipoprotein A-I modulates regulatory T cells in autoimmune ldlr−/−, apoA-I−/− mice. *J. Biol. Chem.* **285:** 36158–36169.

26. Bhat, S., M. G. Sorci-Thomas, and M. J. Thomas. 2005. Intermolecular contact between globular N-terminal fold and C-terminal Domain of ApoA-I stabilizes its lipid-bound conformation: studies employing chemical cross-linking and mass spectrometry. *J. Biol. Chem.* **280:** 33015–33025.

27. Bhat, S., M. G. Sorci-Thomas, L. Calabresi, M. P. Samuel, and M. J. Thomas. 2010. Conformation of dimeric apolipoprotein A-Imilano on recombinant lipoprotein particles. *Biochemistry.* **49:** 5213–5224.

28. Berdyshev, E. V., I. A. Gorshkova, J. G. Garcia, V. Natarajan, and W. C. Hubbard. 2005. Quantitative analysis of sphingoid base-1-phosphates as bisacetylated derivatives by liquid chromatography-tandem mass spectrometry. *Anal. Biochem.* **339:** 129–136.

29. Liu, M., J. Seo, J. Allegood, X. Bi, X. Zhu, E. Boudyguina, A. K. Gebre, D. Shah, M. G. Sorci-Thomas, M. J. Thomas, et al. 2013. Hepatic apoM stimulates formation of large, S1P-enriched HDL. *J. Biol. Chem.* **289:** 2801–2814.

30. Wilson, P. C., M. H. Lee, K. M. Appleton, H. M. El-Shewy, T. A. Morinelli, Y. K. Peterson, L. M. Luttrell, and A. A. Jaffa. 2013. The arrestin-selective angiotensin AT1 receptor agonist [Sar1,Ile4,Ile8]-AngII negatively regulates bradykinin B2 receptor signaling via AT1–B2 receptor heterodimers. *J. Biol. Chem.* **288:** 18872–18884.

31. Appleton, K. M., M. H. Lee, C. Alele, C. Alele, D. K. Luttrell, Y. K. Peterson, T. A. Morinelli, and L. M. Luttrell. 2013. Biasing the para-thyroid hormone receptor: relating in vitro ligand efficacy to in vivo biological activity. *Methods Enzymol.* **522:** 229–262.

32. Leonard, A. P., K. M. Appleton, L. M. Luttrell, and Y. K. Peterson. 2013. A high-content, live-cell, and real-time approach to the quantitation of ligand-induced β-Arrestin2 and Class A/Class B GPCR mobilization. *Microsc. Microanal.* **19:** 150–170.

33. Bochkov, V., V. Tkachuk, F. Buhler, and T. Resink. 1992. Phosphoinositide and calcium signalling responses in smooth muscle cells: comparison between lipoproteins, Ang II, and PDGF. *Biochem. Biophys. Res. Commun.* **188:** 1295–1304.

34. Honda, H. M., B. K. Wakamatsu, J. I. Goldhaber, J. A. Berliner, M. Navab, and J. N. Weiss. 1999. High-density lipoprotein increases intracellular calcium levels by releasing calcium from internal stores in human endothelial cells. *Atherosclerosis.* **143:** 299–306.

35. Pyne, S., and N. Pyne. 2000. Sphingosine 1-phosphate signalling via the endothelial differentiation gene family of G-protein-coupled receptors. *Pharmacol. Ther.* **88:** 115–131.

36. Van Brocklyn, J. R., M. J. Lee, R. Menzeleev, A. Olivera, L. Edsall, O. Cuvillier, D. M. Thomas, P. J. P. Coopman, S. Thangada, C. H. Liu, T. Hla, and S. Spiegel. 1998. Dual actions of sphingosine 1-phosphate: extracellular through the Gi-coupled receptor EDG1 and intracellular to regulate proliferation and survival. *J. Cell Biol.* **142:** 229–240.

37. Gaborik, Z., and L. Hunyady. 2004. Intracellular trafficking of hormone receptors. *Trends Endocrinol. Metab.* **15:** 286–293.

38. Yuhanna, I. S., Y. Zhu, B. E. Cox, L. D. Hahner, S. Osborne-Lawrence, P. Lu, Y. L. Marcel, R. G. Anderson, M. E. Mendelsohn, H. H. Hobbs, et al. 2001. High-density lipoprotein binding to scavenger receptor-BI activates endothelial nitric oxide synthase. *Nat. Med.* **7:** 853–857.

39. Li, X. A., W. B. Titlow, B. A. Jackson, N. Giltiay, M. Nikolova-Karakashian, A. Uittenbogaard, and E. J. Smart. 2002. High density lipoprotein binding to scavenger receptor, Class B, type I activates endothelial nitric-oxide synthase in a ceramide-dependent manner. *J. Biol. Chem.* **277:** 11058–11063.

40. Kocher, O., A. Yesilaltay, C. Cirovic, R. Pal, A. Rigotti, and M. Krieger. 2003. Targeted disruption of the PDZK1 gene in mice causes tissue-specific depletion of the high density lipoprotein receptor scavenger receptor class B type I and altered lipoprotein metabolism. *J. Biol. Chem.* **278:** 52820–52825.

41. Assanasen, C., C. Mineo, D. Seetharam, I. S. Yuhanna, Y. L. Marcel, M. A. Connelly, D. L. Williams, M. de la Llera-Moya, P. W. Shaul, and D. L. Silver. 2005. Cholesterol binding, efflux, and a PDZ-interacting domain of scavenger receptor-BI mediate HDL-initiated signaling. *J. Clin. Invest.* **115:** 969–977.

42. Rentero, C., R. Evans, P. Wood, F. Tebar, S. Vila de Muga, L. Cubells, I. de Diego, T. E. Hayes, W. E. Hughes, A. Pol, et al. 2006. Inhibition of H-Ras and MAPK is compensated by PKC-dependent pathways in annexin A6 expressing cells. *Cell. Signal.* **18:** 1006–1016.

43. Eckhardt, E. R., L. Cai, B. Sun, N. R. Webb, and D. R. van der Westhuyzen. 2004. High density lipoprotein uptake by scavenger receptor SR-BII. *J. Biol. Chem.* **279:** 14372–14381.

44. Peng, Y., W. Akmentin, M. A. Connelly, S. Lund-Katz, M. C. Phillips, and D. L. Williams. 2004. Scavenger receptor BI (SR-BI) clustered on microvillar extensions suggests that this plasma membrane domain is a way station for cholesterol trafficking between cells and high-density lipoprotein. *Mol. Biol. Cell.* **15:** 384–396.

45. Stefan, E., S. Aquin, N. Berger, C. R. Landry, B. Nyfeler, M. Bouvier, and S. W. Michnick. 2007. Quantification of dynamic protein complexes using Renilla luciferase fragment complementation applied to protein kinase A activities in vivo. *Proc. Natl. Acad. Sci. USA.* **104:** 16916–16921.

46. Babitt, J., B. Trigatti, A. Rigotti, E. J. Smart, R. G. Anderson, S. Xu, and M. Krieger. 1997. Murine SR-BI, a high density lipoprotein receptor that mediates selective lipid uptake, is N-glycosylated and fatty acylated and colocalizes with plasma membrane caveolae. *J. Biol. Chem.* **272:** 13242–13249.

47. Tondu, A. L., C. Robichon, L. Yvan-Charvet, N. Donne, X. Le Liepvre, E. Hajduch, P. Ferre, I. Dugail, and G. Dagher. 2005. Insulin and angiotensin II induce the translocation of scavenger receptor class B, type I from intracellular sites to the plasma membrane of adipocytes. *J. Biol. Chem.* **280:** 33536–33540.

48. Potì, F., M. Simoni, and J. R. Nofer. 2014. Atheroprotective role of high-density lipoprotein (HDL)-associated sphingosine-1-phosphate (S1P). *Cardiovasc. Res.* **103:** 395–404.

49. Liu, X., S. L. Xion, and G. H. Yi. 2012. ABCA1, ABCG1, and SR-BI: Transit of HDL-associated sphingosine-1-phosphate. *Clin. Chim. Acta.* **413:** 384–390.

50. Pollard, R. D., C. N. Blesso, M. Zabalawi, B. Fulp, M. Gerelu, X. Zhu, E. W. Lyons, N. Nuradin, O. L. Francone, X. A. Li, et al. 2015. Procollagen C-endopeptidase enhancer protein 2 (PCPE2) reduces atherosclerosis in mice by enhancing scavenger receptor class B1 (SR-BI)-mediated high-density lipoprotein (HDL)-cholesteryl ester uptake. *J. Biol. Chem.* **290:** 15496–15511.

51. Tatematsu, S., S. A. Francis, P. Natarajan, D. J. Rader, A. Saghatelian, J. D. Brown, T. Michel, and J. Plutzky. 2013. Endothelial lipase is a critical determinant of high-density lipoprotein-stimulated sphingosine 1-phosphate-dependent signaling in vascular endothelium. *Arteriosl. Thromb. Vasc Biol.* **33:** 1788–1794.

52. Christoffersen, C., H. Obinata, S. B. Kumaraswamy, S. Galvani, J. Ahnström, M. Sevvana, C. Egerer-Sieber, Y. A. Muller, T. Hla, L. B. Nielsen, et al. 2011. Endothelium-protective sphingosine-1-phosphate provided by HDL-associated apolipoprotein M. *Proc. Natl. Acad. Sci. USA.* **108:** 9613–9618.

53. Galvani, S., M. Sanson, V. A. Blaho, S. L. Swendeman, H. Conger, B. Dahlbäck, M. Kono, R. L. Proia, J. D. Smith, and T. Hla. 2015. HDL-bound sphingosine 1-phosphate acts as a biased agonist for the endothelial cell receptor S1P1 to limit vascular inflammation. *Sci. Signal.* **8:** ra79.

54. Sattler, K., M. Gräler, P. Keul, S. Weske, C. M. Reimann, H. Jindrová, P. Kleinbongard, R. Sabbadini, M. Bröcker-Preuss, R. Erbel, et al. 2015. Defects of high-density lipoproteins in coronary artery disease caused by low sphingosine-1-phosphate content: correction by sphingosine-1-phosphate-loading. *J. Am. Coll. Cardiol.* **66:** 1470–1485.

55. Karuna, R., R. Park, A. Othman, A. G. Holleboom, M. M. Motazacker, I. Sutter, J. A. Kuivenhoven, L. Rohrer, H. Matile, T. Hornemann, et al. 2011. Plasma levels of sphingosine-1-phosphate and apolipoprotein M in patients with monogenic disorders of HDL metabolism. *Atherosclerosis.* **219:** 855–863.

56. Hammad, S. M., S. Stefansson, W. O. Twal, C. J. Drake, P. Fleming, A. Remaley, H. B. Brewer, Jr., and W. S. Argraves. 1999. Cubilin, the endocytic receptor for intrinsic factor-vitamin B(12) complex, mediates high-density lipoprotein holoparticle endocytosis. *Proc. Natl. Acad. Sci. USA.* **96:** 10158–10163.

57. Fidge, N. H. 1999. High density lipoprotein receptors, binding proteins, and ligands. *J. Lipid Res.* **40:** 187–201.